Observation of the Decay $B^0 \rightarrow \rho^+\rho^-$ and Measurement of the Branching Fraction and Polarization

The *BABAR* Collaboration

August 9, 2003

Abstract

We have observed the rare decay $B^0 \rightarrow \rho^+\rho^-$ in a sample of 89 million $B\overline{B}$ pairs recorded with the *BABAR* detector. We measure the branching fraction $\mathcal{B}(B^0 \rightarrow \rho^+\rho^-) = (27^{+7+5}_{-6-7}) \times 10^{-6}$ and determine the longitudinal polarization fraction $\Gamma_L/\Gamma = 0.99^{+0.01}_{-0.07} \pm 0.03$. Our results are preliminary.

Contributed to the XXIst International Symposium on Lepton and Photon Interactions at High Energies, 8/11 — 8/16/2003, Fermilab, Illinois USA

The *BABAR* Collaboration,

B. Aubert, R. Barate, D. Boutigny, J.-M. Gaillard, A. Hicheur, Y. Karyotakis, J. P. Lees, P. Robbe,
V. Tisserand, A. Zghiche

Laboratoire de Physique des Particules, F-74941 Annecy-le-Vieux, France

A. Palano, A. Pompili

Università di Bari, Dipartimento di Fisica and INFN, I-70126 Bari, Italy

J. C. Chen, N. D. Qi, G. Rong, P. Wang, Y. S. Zhu

Institute of High Energy Physics, Beijing 100039, China

G. Eigen, I. Ofte, B. Stugu

University of Bergen, Inst. of Physics, N-5007 Bergen, Norway

G. S. Abrams, A. W. Borgland, A. B. Breon, D. N. Brown, J. Button-Shafer, R. N. Cahn, E. Charles,
C. T. Day, M. S. Gill, A. V. Gritsan, Y. Groysman, R. G. Jacobsen, R. W. Kadel, J. Kadyk, L. T. Kerth,
Yu. G. Kolomensky, J. F. Kral, G. Kukartsev, C. LeClerc, M. E. Levi, G. Lynch, L. M. Mir, P. J. Oddone,
T. J. Orimoto, M. Pripstein, N. A. Roe, A. Romosan, M. T. Ronan, V. G. Shelkov, A. V. Telnov,
W. A. Wenzel

Lawrence Berkeley National Laboratory and University of California, Berkeley, CA 94720, USA

K. Ford, T. J. Harrison, C. M. Hawkes, D. J. Knowles, S. E. Morgan, R. C. Penny, A. T. Watson,
N. K. Watson

University of Birmingham, Birmingham, B15 2TT, United Kingdom

T. Held, K. Goetzen, H. Koch, B. Lewandowski, M. Pelizaeus, K. Peters, H. Schmuecker, M. Steinke

Ruhr Universität Bochum, Institut für Experimentalphysik 1, D-44780 Bochum, Germany

N. R. Barlow, J. T. Boyd, N. Chevalier, W. N. Cottingham, M. P. Kelly, T. E. Latham, C. Mackay,
F. F. Wilson

University of Bristol, Bristol BS8 1TL, United Kingdom

K. Abe, T. Cuhadar-Donszelmann, C. Hearty, T. S. Mattison, J. A. McKenna, D. Thiessen

University of British Columbia, Vancouver, BC, Canada V6T 1Z1

P. Kyberd, A. K. McKemey

Brunel University, Uxbridge, Middlesex UB8 3PH, United Kingdom

V. E. Blinov, A. D. Bukin, V. B. Golubev, V. N. Ivanchenko, E. A. Kravchenko, A. P. Onuchin,
S. I. Serednyakov, Yu. I. Skovpen, E. P. Solodov, A. N. Yushkov

Budker Institute of Nuclear Physics, Novosibirsk 630090, Russia

D. Best, M. Bruinsma, M. Chao, D. Kirkby, A. J. Lankford, M. Mandelkern, R. K. Mommsen, W. Roethel,
D. P. Stoker

University of California at Irvine, Irvine, CA 92697, USA

C. Buchanan, B. L. Hartfiel

University of California at Los Angeles, Los Angeles, CA 90024, USA

B. C. Shen

University of California at Riverside, Riverside, CA 92521, USA

D. del Re, H. K. Hadavand, E. J. Hill, D. B. MacFarlane, H. P. Paar, Sh. Rahatlou, V. Sharma

University of California at San Diego, La Jolla, CA 92093, USA

J. W. Berryhill, C. Campagnari, B. Dahmes, N. Kuznetsova, S. L. Levy, O. Long, A. Lu, M. A. Mazur, J. D. Richman, W. Verkerke

University of California at Santa Barbara, Santa Barbara, CA 93106, USA

T. W. Beck, J. Beringer, A. M. Eisner, C. A. Heusch, W. S. Lockman, T. Schalk, R. E. Schmitz, B. A. Schumm, A. Seiden, M. Turri, W. Walkowiak, D. C. Williams, M. G. Wilson

University of California at Santa Cruz, Institute for Particle Physics, Santa Cruz, CA 95064, USA

J. Albert, E. Chen, G. P. Dubois-Felsmann, A. Dvoretskii, D. G. Hitlin, I. Narsky, F. C. Porter, A. Ryd, A. Samuel, S. Yang

California Institute of Technology, Pasadena, CA 91125, USA

S. Jayatilleke, G. Mancinelli, B. T. Meadows, M. D. Sokoloff

University of Cincinnati, Cincinnati, OH 45221, USA

T. Abe, F. Blanc, P. Bloom, S. Chen, P. J. Clark, W. T. Ford, U. Nauenberg, A. Olivas, P. Rankin, J. Roy, J. G. Smith, W. C. van Hoek, L. Zhang

University of Colorado, Boulder, CO 80309, USA

J. L. Harton, T. Hu, A. Soffer, W. H. Toki, R. J. Wilson, J. Zhang

Colorado State University, Fort Collins, CO 80523, USA

D. Altenburg, T. Brandt, J. Brose, T. Colberg, M. Dickopp, R. S. Dubitzky, A. Hauke, H. M. Lacker, E. Maly, R. Müller-Pfefferkorn, R. Nogowski, S. Otto, J. Schubert, K. R. Schubert, R. Schwierz, B. Spaan, L. Wilden

Technische Universität Dresden, Institut für Kern- und Teilchenphysik, D-01062 Dresden, Germany

D. Bernard, G. R. Bonneaud, F. Brochard, J. Cohen-Tanugi, P. Grenier, Ch. Thiebaux, G. Vasileiadis, M. Verderi

Ecole Polytechnique, LLR, F-91128 Palaiseau, France

A. Khan, D. Lavin, F. Muheim, S. Playfer, J. E. Swain

University of Edinburgh, Edinburgh EH9 3JZ, United Kingdom

M. Andreotti, V. Azzolini, D. Bettoni, C. Bozzi, R. Calabrese, G. Cibinetto, E. Luppi, M. Negrini, L. Piemontese, A. Sarti

Università di Ferrara, Dipartimento di Fisica and INFN, I-44100 Ferrara, Italy

E. Treadwell

Florida A&M University, Tallahassee, FL 32307, USA

F. Anulli,[1] R. Baldini-Ferroli, M. Biasini,[1] A. Calcaterra, R. de Sangro, D. Falciai, G. Finocchiaro, P. Patteri, I. M. Peruzzi,[1] M. Piccolo, M. Pioppi,[1] A. Zallo

Laboratori Nazionali di Frascati dell'INFN, I-00044 Frascati, Italy

---

[1]Also with Università di Perugia, Perugia, Italy

3

A. Buzzo, R. Capra, R. Contri, G. Crosetti, M. Lo Vetere, M. Macri, M. R. Monge, S. Passaggio, C. Patrignani, E. Robutti, A. Santroni, S. Tosi

Università di Genova, Dipartimento di Fisica and INFN, I-16146 Genova, Italy

S. Bailey, M. Morii, E. Won

Harvard University, Cambridge, MA 02138, USA

W. Bhimji, D. A. Bowerman, P. D. Dauncey, U. Egede, I. Eschrich, J. R. Gaillard, G. W. Morton, J. A. Nash, P. Sanders, G. P. Taylor

Imperial College London, London, SW7 2BW, United Kingdom

G. J. Grenier, S.-J. Lee, U. Mallik

University of Iowa, Iowa City, IA 52242, USA

J. Cochran, H. B. Crawley, J. Lamsa, W. T. Meyer, S. Prell, E. I. Rosenberg, J. Yi

Iowa State University, Ames, IA 50011-3160, USA

M. Davier, G. Grosdidier, A. Höcker, S. Laplace, F. Le Diberder, V. Lepeltier, A. M. Lutz, T. C. Petersen, S. Plaszczynski, M. H. Schune, L. Tantot, G. Wormser

Laboratoire de l'Accélérateur Linéaire, F-91898 Orsay, France

V. Brigljević , C. H. Cheng, D. J. Lange, D. M. Wright

Lawrence Livermore National Laboratory, Livermore, CA 94550, USA

A. J. Bevan, J. P. Coleman, J. R. Fry, E. Gabathuler, R. Gamet, M. Kay, R. J. Parry, D. J. Payne, R. J. Sloane, C. Touramanis

University of Liverpool, Liverpool L69 3BX, United Kingdom

J. J. Back, P. F. Harrison, H. W. Shorthouse, P. Strother, P. B. Vidal

Queen Mary, University of London, E1 4NS, United Kingdom

C. L. Brown, G. Cowan, R. L. Flack, H. U. Flaecher, S. George, M. G. Green, A. Kurup, C. E. Marker, T. R. McMahon, S. Ricciardi, F. Salvatore, G. Vaitsas, M. A. Winter

University of London, Royal Holloway and Bedford New College, Egham, Surrey TW20 0EX, United Kingdom

D. Brown, C. L. Davis

University of Louisville, Louisville, KY 40292, USA

J. Allison, R. J. Barlow, A. C. Forti, P. A. Hart, M. C. Hodgkinson, F. Jackson, G. D. Lafferty, A. J. Lyon, J. H. Weatherall, J. C. Williams

University of Manchester, Manchester M13 9PL, United Kingdom

A. Farbin, A. Jawahery, D. Kovalskyi, C. K. Lae, V. Lillard, D. A. Roberts

University of Maryland, College Park, MD 20742, USA

G. Blaylock, C. Dallapiccola, K. T. Flood, S. S. Hertzbach, R. Kofler, V. B. Koptchev, T. B. Moore, S. Saremi, H. Staengle, S. Willocq

University of Massachusetts, Amherst, MA 01003, USA

4

R. Cowan, G. Sciolla, F. Taylor, R. K. Yamamoto

Massachusetts Institute of Technology, Laboratory for Nuclear Science, Cambridge, MA 02139, USA

D. J. J. Mangeol, P. M. Patel

McGill University, Montréal, QC, Canada H3A 2T8

A. Lazzaro, F. Palombo

Università di Milano, Dipartimento di Fisica and INFN, I-20133 Milano, Italy

J. M. Bauer, L. Cremaldi, V. Eschenburg, R. Godang, R. Kroeger, J. Reidy, D. A. Sanders, D. J. Summers, H. W. Zhao

University of Mississippi, University, MS 38677, USA

S. Brunet, D. Cote-Ahern, C. Hast, P. Taras

Université de Montréal, Laboratoire René J. A. Lévesque, Montréal, QC, Canada H3C 3J7

H. Nicholson

Mount Holyoke College, South Hadley, MA 01075, USA

C. Cartaro, N. Cavallo,[2] G. De Nardo, F. Fabozzi,[2] C. Gatto, L. Lista, P. Paolucci, D. Piccolo, C. Sciacca

Università di Napoli Federico II, Dipartimento di Scienze Fisiche and INFN, I-80126, Napoli, Italy

M. A. Baak, G. Raven

NIKHEF, National Institute for Nuclear Physics and High Energy Physics, NL-1009 DB Amsterdam, The Net herlands

J. M. LoSecco

University of Notre Dame, Notre Dame, IN 46556, USA

T. A. Gabriel

Oak Ridge National Laboratory, Oak Ridge, TN 37831, USA

B. Brau, K. K. Gan, K. Honscheid, D. Hufnagel, H. Kagan, R. Kass, T. Pulliam, Q. K. Wong

Ohio State University, Columbus, OH 43210, USA

J. Brau, R. Frey, C. T. Potter, N. B. Sinev, D. Strom, E. Torrence

University of Oregon, Eugene, OR 97403, USA

F. Colecchia, A. Dorigo, F. Galeazzi, M. Margoni, M. Morandin, M. Posocco, M. Rotondo, F. Simonetto, R. Stroili, G. Tiozzo, C. Voci

Università di Padova, Dipartimento di Fisica and INFN, I-35131 Padova, Italy

M. Benayoun, H. Briand, J. Chauveau, P. David, Ch. de la Vaissière, L. Del Buono, O. Hamon, M. J. J. John, Ph. Leruste, J. Ocariz, M. Pivk, L. Roos, J. Stark, S. T'Jampens, G. Therin

Universités Paris VI et VII, Lab de Physique Nucléaire H. E., F-75252 Paris, France

P. F. Manfredi, V. Re

Università di Pavia, Dipartimento di Elettronica and INFN, I-27100 Pavia, Italy

---

[2]Also with Università della Basilicata, Potenza, Italy

P. K. Behera, L. Gladney, Q. H. Guo, J. Panetta

University of Pennsylvania, Philadelphia, PA 19104, USA

C. Angelini, G. Batignani, S. Bettarini, M. Bondioli, F. Bucci, G. Calderini, M. Carpinelli, V. Del Gamba, F. Forti, M. A. Giorgi, A. Lusiani, G. Marchiori, F. Martinez-Vidal,[3] M. Morganti, N. Neri, E. Paoloni, M. Rama, G. Rizzo, F. Sandrelli, J. Walsh

Università di Pisa, Dipartimento di Fisica, Scuola Normale Superiore and INFN, I-56127 Pisa, Italy

M. Haire, D. Judd, K. Paick, D. E. Wagoner

Prairie View A&M University, Prairie View, TX 77446, USA

N. Danielson, P. Elmer, C. Lu, V. Miftakov, J. Olsen, A. J. S. Smith, H. A. Tanaka E. W. Varnes

Princeton University, Princeton, NJ 08544, USA

F. Bellini, G. Cavoto,[4] R. Faccini,[5] F. Ferrarotto, F. Ferroni, M. Gaspero, M. A. Mazzoni, S. Morganti, M. Pierini, G. Piredda, F. Safai Tehrani, C. Voena

Università di Roma La Sapienza, Dipartimento di Fisica and INFN, I-00185 Roma, Italy

S. Christ, G. Wagner, R. Waldi

Universität Rostock, D-18051 Rostock, Germany

T. Adye, N. De Groot, B. Franek, N. I. Geddes, G. P. Gopal, E. O. Olaiya, S. M. Xella

Rutherford Appleton Laboratory, Chilton, Didcot, Oxon, OX11 0QX, United Kingdom

R. Aleksan, S. Emery, A. Gaidot, S. F. Ganzhur, P.-F. Giraud, G. Hamel de Monchenault, W. Kozanecki, M. Langer, M. Legendre, G. W. London, B. Mayer, G. Schott, G. Vasseur, M. Zito

DSM/Dapnia, CEA/Saclay, F-91191 Gif-sur-Yvette, France

M. V. Purohit, A. W. Weidemann, F. X. Yumiceva

University of South Carolina, Columbia, SC 29208, USA

D. Aston, R. Bartoldus, N. Berger, A. M. Boyarski, O. L. Buchmueller, M. R. Convery, D. P. Coupal, D. Dong, J. Dorfan, D. Dujmic, W. Dunwoodie, R. C. Field, T. Glanzman, S. J. Gowdy, E. Grauges-Pous, T. Hadig, V. Halyo, T. Hryn'ova, W. R. Innes, C. P. Jessop, M. H. Kelsey, P. Kim, M. L. Kocian, U. Langenegger, D. W. G. S. Leith, S. Luitz, V. Luth, H. L. Lynch, H. Marsiske, R. Messner, D. R. Muller, C. P. O'Grady, V. E. Ozcan, A. Perazzo, M. Perl, S. Petrak, B. N. Ratcliff, S. H. Robertson, A. Roodman, A. A. Salnikov, R. H. Schindler, J. Schwiening, G. Simi, A. Snyder, A. Soha, J. Stelzer, D. Su, M. K. Sullivan, J. Va'vra, S. R. Wagner, M. Weaver, A. J. R. Weinstein, W. J. Wisniewski, D. H. Wright, C. C. Young

Stanford Linear Accelerator Center, Stanford, CA 94309, USA

P. R. Burchat, A. J. Edwards, T. I. Meyer, B. A. Petersen, C. Roat

Stanford University, Stanford, CA 94305-4060, USA

S. Ahmed, M. S. Alam, J. A. Ernst, M. Saleem, F. R. Wappler

State Univ. of New York, Albany, NY 12222, USA

---

[3]Also with IFIC, Instituto de Física Corpuscular, CSIC-Universidad de Valen cia, Valencia, Spain
[4]Also with Princeton University
[5]Also with University of California at San Diego

W. Bugg, M. Krishnamurthy, S. M. Spanier

University of Tennessee, Knoxville, TN 37996, USA

R. Eckmann, H. Kim, J. L. Ritchie, R. F. Schwitters

University of Texas at Austin, Austin, TX 78712, USA

J. M. Izen, I. Kitayama, X. C. Lou, S. Ye

University of Texas at Dallas, Richardson, TX 75083, USA

F. Bianchi, M. Bona, F. Gallo, D. Gamba

Università di Torino, Dipartimento di Fisica Sperimentale and INFN, I-10125 Torino, Italy

C. Borean, L. Bosisio, G. Della Ricca, S. Dittongo, S. Grancagnolo, L. Lanceri, P. Poropat,[6] L. Vitale,
G. Vuagnin

Università di Trieste, Dipartimento di Fisica and INFN, I-34127 Trieste, Italy

R. S. Panvini

Vanderbilt University, Nashville, TN 37235, USA

Sw. Banerjee, C. M. Brown, D. Fortin, P. D. Jackson, R. Kowalewski, J. M. Roney

University of Victoria, Victoria, BC, Canada V8W 3P6

H. R. Band, S. Dasu, M. Datta, A. M. Eichenbaum, J. R. Johnson, P. E. Kutter, H. Li, R. Liu,
F. Di Lodovico, A. Mihalyi, A. K. Mohapatra, Y. Pan, R. Prepost, S. J. Sekula, J. H. von
Wimmersperg-Toeller, J. Wu, S. L. Wu, Z. Yu

University of Wisconsin, Madison, WI 53706, USA

H. Neal

Yale University, New Haven, CT 06511, USA

---

[6]Deceased

1 INTRODUCTION

Charmless B meson decays provide an opportunity to measure the weak-interaction phases arising from the elements of the Cabibbo-Kobayashi-Maskawa (CKM) quark-mixing matrix [1]. There has been increasing interest in the study of $B \to \pi\pi$ and $\rho\pi$ decays where the time-dependent CP-violating asymmetries are related to CKM angle $\alpha \equiv \arg\left[-V_{td}V_{tb}^* / V_{ud}V_{ub}^*\right]$ and interference between the tree and penguin amplitudes could give rise to direct-CP violation. The decay[7] $B^0 \to \rho^+\rho^-$ is another promising mode for CP violation studies and constraints on the angle α. The angular correlations in this decay to two vector particles introduce additional complications in the analysis, but the measurement of the magnitudes or phases of the helicity amplitudes will provide better understanding of the decay models [2, 3, 4].

The decay $B^0 \to \rho^+\rho^-$ is expected to proceed through tree-level $b \to u$ transitions and CKM-suppressed $b \to d$ penguins as illustrated in Fig. 1. The presence of penguins and both CP-even
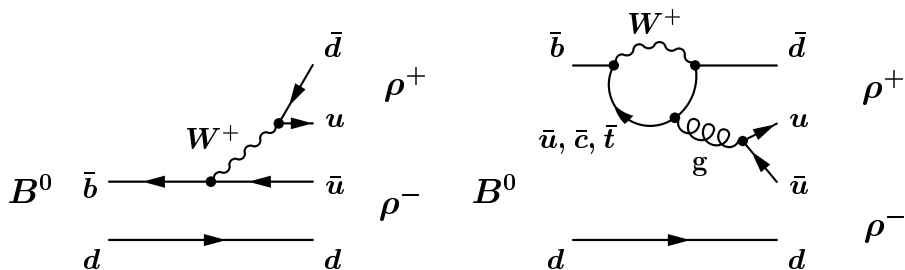

Figure 1: *Two of the diagrams describing the decays $B^0 \to \rho^+\rho^-$.*

(S- and D-wave) and CP-odd (P-wave) components in the decay amplitude complicate the measurement of α. Isospin relations among the three $B \to \rho\rho$ modes may reduce the uncertainties in the measurement of α due to penguin contributions (penguin pollution), analogous to the methods proposed for $B \to \pi\pi$ [5]. The recent limit on the $B^0 \to \rho^0\rho^0$ decay rate [6] and the measurements of the $B^+ \to \rho^+\rho^0$ branching fraction [6, 7] result in experimental limits on the amount of penguin pollution, while $B^+ \to \rho^+\rho^0$ polarization measurements provide evidence that the CP-even longitudinal component dominates in the $B \to \rho\rho$ decay amplitudes. In this paper we report on the observation of the $B^0 \to \rho^+\rho^-$ decay mode and the measurement of its branching fraction and the longitudinal polarization fraction in the decay.

2 THE *BABAR* DETECTOR AND DATASET

In this analysis, we use the data collected with the *BABAR* detector [8] at the PEP-II asymmetric-energy e^+e^- collider [9] operated at the center-of-mass (CM) energy of the $\Upsilon(4S)$ resonance ($\sqrt{s} = 10.58$ GeV). These data represent an integrated luminosity of 81.9 fb^{-1}, corresponding to 88.9 million $B\overline{B}$ pairs, at the $\Upsilon(4S)$ energy (on-resonance) and 9.6 fb^{-1} approximately 40 MeV below this energy (off-resonance).

Charged-particle momenta are measured in a tracking system consisting a five-layer double-sided silicon vertex tracker (SVT) and a 40-layer central drift chamber (DCH), both immersed in a

---

[7]Charge conjugation is implied here and throughout this paper unless explicitly stated.

1.5 T axial magnetic field. *BABAR* achieves an impact parameter resolution of about 40 μm for the high momentum charged particles in the B decay final states, allowing the precise determination of decay vertices. The tracking system covers 92% of the solid angle in the CM frame.

Charged-particle identification is provided by measurements of the energy loss (dE/dx) in the tracking devices (SVT and DCH) and by an internally reflecting ring-imaging Cherenkov detector (DIRC) covering the central region. A K-π separation of better than four standard deviations (σ) is achieved for momenta below 3 GeV/c, decreasing to 2.5 σ at the highest momenta in the B decay final states. Photons are detected by a CsI(Tl) electromagnetic calorimeter (EMC). The EMC provides good energy and angular resolution for detection of photons in the range from 20 MeV to 4 GeV. The energy and angular resolutions are 3% and 4 mrad, respectively, for a 1 GeV photon.

3 EVENT SELECTION

Hadronic events are selected based on track multiplicity and event topology. We fully reconstruct $B^0 \to \rho^+\rho^-$ candidates from their decay products $\rho^\pm \to \pi^\pm\pi^0$ and $\pi^0 \to \gamma\gamma$. Charged track candidates are required to originate from the interaction point, and to have at least 12 DCH hits and a minimum transverse momentum of 0.1 GeV/c. Charged pion tracks are distinguished from kaon and proton tracks via a likelihood ratio that includes dE/dx information from the SVT and DCH for momenta below 0.7 GeV/c and the DIRC Cherenkov angle and number of photons for higher momenta. They are also distinguished from electrons primarily on the basis of the EMC shower energy and lateral shower moments.

We reconstruct π^0 mesons from pairs of photons, each with a minimum energy of 30 MeV, with the shower shape consistent with the photon hypothesis, and not matched to a track. The typical width of the reconstructed π^0 mass is 7 MeV. We accept π^0 candidates in the invariant mass interval ± 15 MeV from the nominal mass. We select ρ candidates to satisfy $0.52 \text{ GeV} < m_{\pi\pi} < 1.02 \text{ GeV}$. The helicity angles θ_1 and θ_2 of ρ^+ and ρ^- are defined as the angles between the π^0 direction in the ρ rest frame and the direction of the ρ boost with respect to the B as shown in Fig. 2. We restrict the helicity angles to the region $-0.75 \leq \cos\theta_{1,2} \leq 0.95$ to suppress combinatorial background and reduce acceptance uncertainties due to low-momentum pion reconstruction.
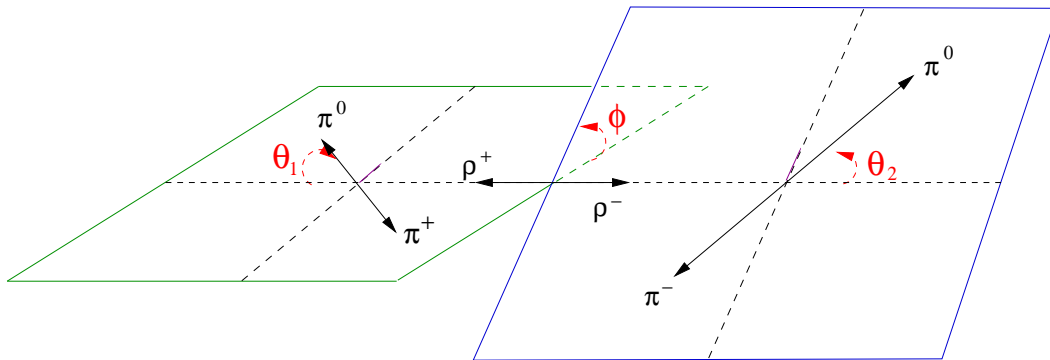

Figure 2: *Definition of helicity angles (θ_1 and θ_2) in $B^0 \to \rho^+\rho^-$ decays.*

To reject the dominant continuum background (from $e^+e^- \to q\bar{q}$ events, $q = u, d, s, c$), we require $|\cos\theta_T| < 0.8$, where θ_T is the angle between the thrust axis of the B candidate and the

thrust axis of the rest of the tracks and neutral clusters in the event, calculated in the CM frame. The distribution of $|\cos\theta_T|$ is sharply peaked near 1 for jet-like events originating from $q\bar{q}$ pairs and nearly uniform for the isotropic decays of the B meson. We also construct a Fisher discriminant ($\mathcal{F}$) that combines 11 variables: the polar angle of the B momentum vector, the polar angle of the B-candidate thrust axis, both calculated with respect to the beam axis in the CM frame, and the scalar sum of the CM momenta of charged particles and photons (excluding particles from the B candidate) entering nine coaxial angular intervals of $10°$ around the B-candidate thrust axis [10].

We identify B meson candidates using two nearly independent kinematic variables [8], the beam energy-substituted mass $m_{\mathrm{ES}} = [(s/2 + \mathbf{p}_i \cdot \mathbf{p}_B)^2/E_i^2 - \mathbf{p}_B^2]^{1/2}$ and the energy difference $\Delta E = (E_i E_B - \mathbf{p}_i \cdot \mathbf{p}_B - s/2)/\sqrt{s}$, where $(E_i, \mathbf{p}_i)$ is the e^+e^- initial state four-momentum, and $(E_B, \mathbf{p}_B)$ is the four-momentum of the reconstructed B candidate, all defined in the laboratory frame. For signal events the m_{ES} distribution peaks at the B mass and the ΔE distribution peaks near zero. Our initial selection requires $m_{\mathrm{ES}} > 5.2$ GeV and $|\Delta E| < 0.2$ GeV, while the signal resolution is roughly 3 MeV and 50 MeV, respectively. The selected sample contains 54042 events most of which are retained in sidebands of the variables for later fitting.

4   ANALYSIS METHOD

We use an unbinned, extended maximum-likelihood (ML) fit to extract simultaneously the signal yield and angular polarization. There are three event yield (n_j) categories j: signal, continuum $q\bar{q}$, and $B\overline{B}$ combinatorial background. We define the likelihood for each $B^0 \to \rho^+\rho^-$ event candidate i:

$$\mathcal{L}_i = \sum_{j=1}^{3} n_j \, \mathcal{P}_j(\vec{x}_i; \vec{\alpha}), \tag{1}$$

where each of the $\mathcal{P}_j(\vec{x}_i; \vec{\alpha})$ is the probability density function (PDF) for measured variables $\vec{x}_i$. The numbers $\vec{\alpha}$ parameterize the expected PDFs of measured variables in each category. We allow for multiple candidates in a given event by assigning to each selected candidate a weight of $1/N_i$, where N_i is the number of candidates in that same event. The average number of candidates per event is 1.27. The extended likelihood for a sample of N_{cand} candidates is

$$\mathcal{L} = \exp\left(-\sum_{j=1}^{3} n_j\right) \prod_{i=1}^{N_{\mathrm{cand}}} \exp\left(\frac{\ln \mathcal{L}_i}{N_i}\right). \tag{2}$$

The seven fit input variables $\vec{x}_i$ are m_{ES}, ΔE, $\mathcal{F}$, invariant masses of the ρ^+ and ρ^- candidates, and the corresponding helicity angles θ_1 and θ_2. The correlations among the fit input variables for the data and signal Monte Carlo (MC) [11] are found to be small (typically less than 5%), except for angular correlations in the signal as discussed below. The PDF, $\mathcal{P}_j(\vec{x}_i; \vec{\alpha})$, for a given candidate i is the product of those for each of the variables and a joint PDF for the helicity angles, which accounts for the angular correlations in the signal and for detector acceptance effects. We integrate over the angle ϕ between the two decay planes shown in Fig. 2, leaving a PDF that depends only on the two helicity angles and the unknown longitudinal polarization fraction $f_L \equiv \Gamma_L/\Gamma$, where Γ_L and Γ are the longitudinal and total decay widths. The differential decay width [2] is defined as:

$$\frac{1}{\Gamma} \frac{\mathrm{d}^2\Gamma}{\mathrm{d}\cos\theta_1 \, \mathrm{d}\cos\theta_2} = \frac{9}{4}\left\{\frac{1}{4}(1 - f_L)\sin^2\theta_1 \sin^2\theta_2 + f_L \cos^2\theta_1 \cos^2\theta_2\right\} . \tag{3}$$

The PDF parameters $\vec{\alpha}$, except for f_L, are extracted from MC simulation and on-resonance m_{ES} and ΔE sidebands. The MC resolutions are adjusted by comparisons of data and simulation in abundant calibration channels with similar kinematics and topology, such as $B \to D\pi, D\rho$ with $D \to K\pi\pi, K\pi$. To describe the signal distributions, we use Gaussian functions for the parameterization of the PDFs for m_{ES} and ΔE, and a relativistic P-wave Breit-Wigner distribution for the ρ resonance masses. The angular acceptance effects are parameterized with empirical polynomial functions for each helicity angle and are included in the joint helicity-angle PDF as a product with ideal distribution in Eq. (3). For the background PDFs, we use polynomials or, in the case of m_{ES}, an empirical phase-space function [12]. In the background PDF we incorporate a small linear correlation between the curvature of the phase-space function and the event shape variable $\mathcal{F}$. The background parameterizations for the ρ candidate masses also include a resonant component to account for ρ production in the continuum. The background helicity-angle distribution is also separated into contributions from combinatorial background and from real ρ mesons, both described by polynomials. The PDF for $\mathcal{F}$ is represented by a Gaussian distribution with different widths above and below the mean for both signal and background.

There is a fraction of incorrectly reconstructed (fake) $B^0 \to \rho^+\rho^-$ events expected in the selected sample. This happens when at least one candidate photon in a π^0 candidate or one charged track in a ρ candidate belongs to the decay tree of the other B. MC simulation shows that about 30% of selected $B^0 \to \rho^+\rho^-$ events with longitudinal polarization do not have the correct decay tree reconstructed, while about 20% of the events have both correctly and incorrectly reconstructed decay candidates. We do not account explicitly for the fake events in the signal PDF parameterization since they introduce substantial tails in the distributions; these tails have weak discrimination power from background and we cannot fully rely on the MC simulation of the fake component distributions. We account for these effects in the signal efficiency evaluation.

MC simulation indicates that about 5% of the events in the final sample are from other B decays. This background, arising mainly from $b \to c$ transitions, is explicitly accounted for in the fit. PDFs for this background are taken from MC including a contribution from charmless decays such as $B \to \rho\pi$, $\rho^0\rho^+$, ρK^*, $a_1\pi$, and $a_1\rho$. The branching fractions for these and many other exclusive modes were taken from the most recent experimental measurements [13] or extrapolated from other results with flavor symmetry approximation. Their contribution was shown to be well accounted for by a single B-background fit component. In this analysis we do not explicitly include a fit component for other partial waves, including non-resonant decays, with the same final-state particles selected within the ρ resonance mass window. These types of decays are assumed to be negligible, they are significantly suppressed by the mass and helicity-angle information in the fit, and they are examined in the mass and helicity-angle distributions as discussed below.

The event yields n_j and polarization f_L are obtained by minimizing the quantity $\chi^2 \equiv -2\ln\mathcal{L}$. The dependence of χ^2 on a fit parameter n_j or f_L is obtained with the other fit parameters floating. We quote statistical errors corresponding to a unit increase in χ^2. The statistical significance of the signal is defined as the square root of the change in χ^2 when constraining the number of signal events to zero in the likelihood fit.

5 PHYSICS RESULTS

The results of our maximum likelihood fits are summarized in Table 1. The statistical significance of the $B^0 \to \rho^+\rho^-$ signal is 5.9 σ. We find that the decay amplitude is predominantly longitudinal. To compute the branching fraction, we assume equal production rates for $B^0\overline{B}^0$ and B^+B^-. To

check the stability of our results we refit removing each variable from the fit and find consistent results. The number of fitted events, statistical significance, branching fraction and polarization measurement errors, and the ML fit χ^2 value are well reproduced with generated MC samples.

The projections of the fit input variables are shown in Fig. 3. The projections are made after a requirement on the signal-to-background probability ratio $\mathcal{P}_{\mathrm{sig}}/\mathcal{P}_{\mathrm{bkg}}$, where $\mathcal{P}_{\mathrm{sig}}$ and $\mathcal{P}_{\mathrm{bkg}}$ are the signal and background PDFs defined in Eq. (1), but with the PDF for the plotted variable excluded. The histograms show the data with about $40-60\%$ of signal retained, the lines show the PDF projections from the full sample. Both mass and helicity-angle projections provide no evidence for non-resonant B decays with the same four-pion final states.

To check the sensitivity of our results to the presence of non-resonant $B^0 \rightarrow \rho^{\pm}\pi^{\mp}\pi^0$ and $B^0 \rightarrow \pi^+\pi^-\pi^0\pi^0$ decays, we explicitly include a fit component assuming phase-space decay model. The selection requirements alone suppress the $B \rightarrow \rho\pi\pi$ (4π) efficiency by one (two) order(s) of magnitude relative to $B^0 \rightarrow \rho^+\rho^-$. The fit results with non-resonant component are consistent with our assumption of negligible non-resonant contribution. We exclude the hypothesis that all the signal is non-resonant $B \rightarrow \rho\pi\pi$ (4π) with 4.7 σ (5.4 σ) statistical significance. However, we cannot exclude that $B \rightarrow \rho\pi\pi$ signal could represent $(9 \pm 15)\%$ (statistical errors only) of our nominal $B^0 \rightarrow \rho^+\rho^-$ event yield, where we ignore interference effects.

Table 1: *A summary of the fit results. The efficiency includes systematic errors, the significance with systematic uncertainties is quoted in parentheses, while for other results, the first error is statistical and the second systematic.*

Reconstruction efficiency	$3.9^{+0.9}_{-0.6}$ %
Signal event yield (n_{sig})	$93^{+23}_{-21} \pm 9$
Statistical significance	5.9 σ (5.3 σ)
Branching fraction $(\mathcal{B})$	$(27\ ^{+7}_{-6}\ ^{+5}_{-7}) \times 10^{-6}$
Signal polarization (f_L)	$0.99\ ^{+0.01}_{-0.07} \pm 0.03$

6   SYSTEMATIC STUDIES

Systematic uncertainties in the ML fit originate from assumptions about the PDF parameters. Uncertainties in the PDF parameters arise from the limited statistics in the background sideband data and signal control samples. We vary them within their respective uncertainties, and derive the associated systematic error on the event yield (9%). The signal remains statistically significant under these variations (5.3 σ including systematics). Additional systematic errors in the number of signal events originate from the uncertainty in the other B-decay cross-feed (3%) that was studied with exclusive MC generated samples.

The systematic errors in the efficiency are due to track finding (2% for two tracks), particle identification (2% for two tracks), and π^0 reconstruction (13% for two π^0s). The efficiency in the ML fit to signal samples, calculated as the ratio of the fit signal yield over the number of fully reconstructed decays in the fit sample, is less than 100% because of fake combinations passing
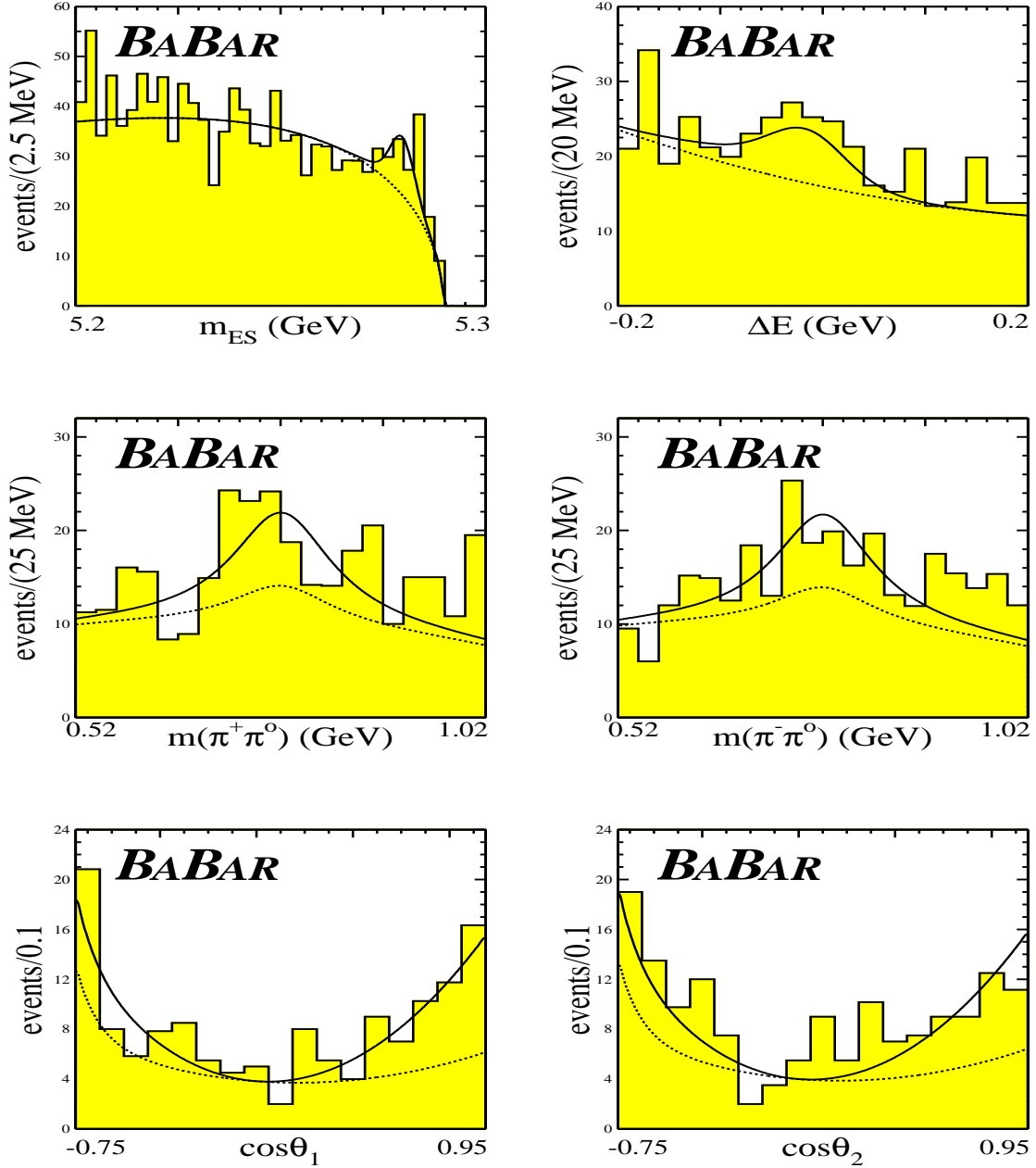
Figure 3: *Projections onto the variables* m_{ES}, ΔE, $m_{\pi^+\pi^0}$, $m_{\pi^-\pi^0}$, $\cos\theta_1$, *and* $\cos\theta_2$ *after a requirement on the signal-to-background probability ratio* $\mathcal{P}_{\mathrm{sig}}/\mathcal{P}_{\mathrm{bkg}}$ *with the PDF for the plotted variable excluded. The histograms show the data, the solid (dashed) line shows the signal-plus-background (background only) PDF projection.*

the selection criteria. We account for this in the efficiency evaluation and assign a systematic uncertainty of 7% taken to be 1/2 of the inefficiency. The reconstruction efficiency depends on the decay polarization. We calculate the efficiencies using the measured polarization and assign a systematic error $\left(^{+17}_{-2}\%\right)$ corresponding to the total polarization measurement error. Smaller systematic uncertainties arise from event-selection criteria, MC statistics, and the number of produced B mesons.

For the polarization measurement, we also include systematic errors from PDF variations that account for uncertainties in the detector acceptance and background parameterizations (0.025). The biases from the resolution in helicity-angle measurement and dilution due to the presence of the fake combinations are studied with MC simulation and are accounted for with a systematic error of 0.02.

7 SUMMARY AND DISCUSSION

We have observed the decay $B^0 \to \rho^+\rho^-$, measured its branching fraction $\mathcal{B} = (27^{+7+5}_{-6-7}) \times 10^{-6}$ and determined the longitudinal polarization fraction $f_L = 0.99^{+0.01}_{-0.07}\pm0.03$. Our results are preliminary. This completes the measurements of the isospin-related $B \to \rho\rho$ modes [6, 7]. The measured branching fraction agrees well with the more recent predictions in the range of $(18$–$35) \times 10^{-6}$ [4], and the suppression of the transverse amplitude (by a factor of m_ρ/m_B) was expected [4]. These measurements improve our understanding of the dynamics of hadronic weak decays and allow experimental tests of effective theories and factorization [2, 3, 4].

The rates of the $B^0 \to \rho^+\rho^-$ and $B^+ \to \rho^0\rho^+$ decays appear to be larger than the corresponding rates of $B \to \pi\pi$ decays [13], while the recent measurement of the $B^+ \to \rho^0 K^{*+}$ branching fraction [6] does not show significant enhancement with respect to $B \to \pi K$ decays [13]. This indicates that the penguin pollution in the $B \to \rho\rho$ decay is smaller than in the $\pi\pi$ case, as predicted prior to the experimental measurements of the $B \to \rho\rho$ modes [3]. The dominance of the CP-even longitudinal polarization in both $B^0 \to \rho^+\rho^-$ and $B^+ \to \rho^0\rho^+$ decays will also simplify CP-violation studies.

At the same time, a relatively smaller experimental limit on the decay rate can be achieved in the $B^0 \to \rho^0\rho^0$ decays than in the $B^0 \to \pi^0\pi^0$ decays, this allows better experimental limit on the amount of penguin pollution in the $B \to \rho\rho$ decay amplitudes. Since the tree contribution for the $B^0 \to \rho^0\rho^0$ decay is color-suppressed, the decay rate is sensitive to the penguin diagram in Fig. 1. Using the earlier *BABAR* measurements [6] we obtain a 90% confidence level upper limit on the ratio of the longitudinal amplitudes A_L in the $B \to \rho\rho$ decays:

$$\frac{|A_L(B^0 \to \rho^0\rho^0)|^2 + |A_L(\overline{B}^0 \to \rho^0\rho^0)|^2}{2 \times |A_L(B^+ \to \rho^0\rho^+)|^2} \equiv \frac{\mathcal{B}(B^0 \to \rho^0\rho^0) \times f_L(B^0 \to \rho^0\rho^0)}{\mathcal{B}(B^+ \to \rho^0\rho^+) \times f_L(B^+ \to \rho^0\rho^+)} < 0.10\,. \quad (4)$$

In the above calculation we assume conservatively the $B^0 \to \rho^0\rho^0$ decay polarization to be fully longitudinal ($f_L = 1$), use the average branching fraction measurements for the B and $\overline{B}$ decays, and assume $|A_L(B^+ \to \rho^0\rho^+)| = |A_L(B^- \to \rho^0\rho^-)|$ with only a tree-diagram contribution. A similar experimental limit for the $B^0 \to \pi^0\pi^0$ and $B^+ \to \pi^+\pi^0$ decay amplitudes is 0.61 [14], though still restrictive on the penguin pollution in the measurement of α [5]. The above observations make the $B^0 \to \rho^+\rho^-$ decay a promising channel to study CP-violation and set constraints on the weak-interaction angle α.

8 ACKNOWLEDGMENTS

References

[1] M. Kobayashi and T. Maskawa, Prog. Theor. Phys. **49**, 652 (1973).

[2] G. Kramer and W.F. Palmer, Phys. Rev. D **45**, 193 (1992).

[3] R. Aleksan *et al.*, Phys. Lett. B **356**, 95 (1995).

[4] D. Ebert, R.N. Faustov, and V.O. Galkin, Phys. Rev. D **56**, 312 (1997); A. Ali, G. Kramer, and C.-D. Lu, Phys. Rev. D **58**, 094009 (1998); Y.-H. Chen *et al.*, Phys. Rev. D **60**, 094014 (1999); H.-Y. Cheng and K.-C. Yang, Phys. Lett. B **511**, 40 (2001).

[5] M. Gronau and D. London, Phys. Rev. Lett. **65**, 3381 (1990); Y. Grossman and H. Quinn, Phys. Rev. D **58**, 017504 (1998).

[6] *BABAR* Collaboration, B. Aubert *et al.*, BABAR-PUB-03-018, hep-ex/0307026, submitted to Phys. Rev. Lett.

[7] BELLE Collaboration, J. Zhang *et al.*, BELLE-2003-6, hep-ex/0306007, submitted to Phys. Rev. Lett.

[8] *BABAR* Collaboration, B. Aubert *et al.*, Nucl. Instrum. Methods **A479**, 1 (2002).

[9] PEP-II Conceptual Design Report, SLAC-R-418 (1993).

[10] CLEO Collaboration, D.M. Asner *et al.*, Phys. Rev. D **53**, 1039 (1996).

[11] The *BABAR* detector Monte Carlo simulation is based on GEANT: R. Brun *et al.*, CERN DD/EE/84-1.

[12] ARGUS Collaboration, H. Albrecht *et al.*, Phys. Lett. B **241**, 278 (1990).

[13] Particle Data Group, K. Hagiwara *et al.*, Phys. Rev. D **66**, 010001 (2002).

[14] *BABAR* Collaboration, B. Aubert *et al.*, Phys. Rev. Lett. **91**, 021801 (2003).